TURBULENT MIXED CONVECTION IN ASYMMETRICALLY HEATED VERTICAL CHANNEL

by

Ameni MOKNI [a,b*], ***Hatem MHIRI*** [b], ***Georges Le PALEC*** [a], ***and Philippe BOURNOT*** [a]

[a] IUSTI UMR CNRS, Technopole de Chateau-Gombert, Marseille, France
[b] Unité de Thermique et Environnement, Ecole Nationale d'Ingénieurs de Monastir, Monastir, Tunisia

Original scientific paper
DOI: 10.2298/TSCI090403018M

In this paper an investigation of mixed convection from vertical heated channel is undertaken. The aim is to explore the heat transfer obtained by adding a forced flow, issued from a flat nozzle located in the entry section of a channel, to the up-going fluid along its walls. Forced and free convection are combined studied in order to increase the cooling requirements. The study deals with both symmetrically and asymmetrically heated channel. The Reynolds number based on the nozzle width and the jet velocity is assumed to be $3\cdot10^3$ and $2\cdot10^4$; whereas, the Rayleigh number based on the channel length and the wall temperature difference varies from $2.57\cdot10^{10}$ to $5.15\cdot10^{12}$. The heating asymmetry effect on the flow development including the mean velocity and temperature, the local Nusselt number, the mass flow rate, and heat transfer are examined.

Key words: *vertical channel, jet, asymmetric heating, mixed convection*

Introduction

Natural convection is unquestionably regarded as a very attractive mode of cooling because of its little cost, minimal maintenance and low noise [1]. As reviewed in [1-3], a substantial body of publications has been documented for the specific case of natural convection in vertical parallel-plate channels with symmetric and asymmetric heating conditions. More recent trends in natural convection research are to improve the heat transfer [4-7] or to analyze standard configurations to carry out optimal geometrical parameters for a better heat transfer rate [8-15]. Adding a forced convection flow is a solution to enhance heat transfer. In many applications although forced convection heat transfer is involved, the effect of buoyancy is not negligible. Such flows are known as "buoyancy affected flows" or more correctly as mixed convection flows. When the Reynolds number (Re) or the Grashof number (Gr) is high enough, the flow is turbulent.

Pioneering work on turbulent mixed convection particularly from vertical tubes has been done by Hall *et al.* [16], Jackson *et al.* [17], and Jiulei *et al*. [18]. Excellent reviews on tur-

* Corresponding author; e-mail: ameni26@yahoo.fr

bulent mixed convection have been done by Jackson *et al*. [19] and Jackson [20]. Nakajima *et al.* [21] studied the effect of buoyancy on the turbulent transport processes in mixed convection for both aiding and opposing flows. Correlations for dimensionless mass flow rate, maximum wall temperature, and average Nusselt number, in terms of Rayleigh number and dimensionless geometric parameters are presented by several authors in order to compute the quantities of engineering interest [22-28].

The present theoretical study is concerned with mixed convection in asymmetrically heated vertical channel submitted to a vertical jet of fresh air entering by the bottom. Numerical results are presented in terms of dimensionless induced mass flow rates and dimensionless wall temperatures for different Rayleigh and two Reynolds numbers. Moreover, Nusselt numbers varying with the dimensionless axial co-ordinate X pave the way for the calculation of the average Nusselt numbers.

Assumptions and governing equations

A computational domain of finite dimension illustrated in fig. 1 is employed to simulate the vertical channel which simulates a chimney. A gas jet is issued from a flat nozzle located at the bottom of the channel. The chimney walls are subject to a constant but not equal heat flux. Numerical results are reported for dry air as coolant. The unconfined airflow lies far away from the region of the disturbance induced by the presence of the jet flow. The channel is long enough that the flow becomes turbulent before the exit. The influence of this forced additional jet is analyzed by using the low Reynolds number k-ε turbulence model. The flow is assumed steady and incompressible. Mixed convection is considered by using the Boussinesq approximation in which the density varies linearly with temperature. Other thermo-physical quantities are assumed to be constant.

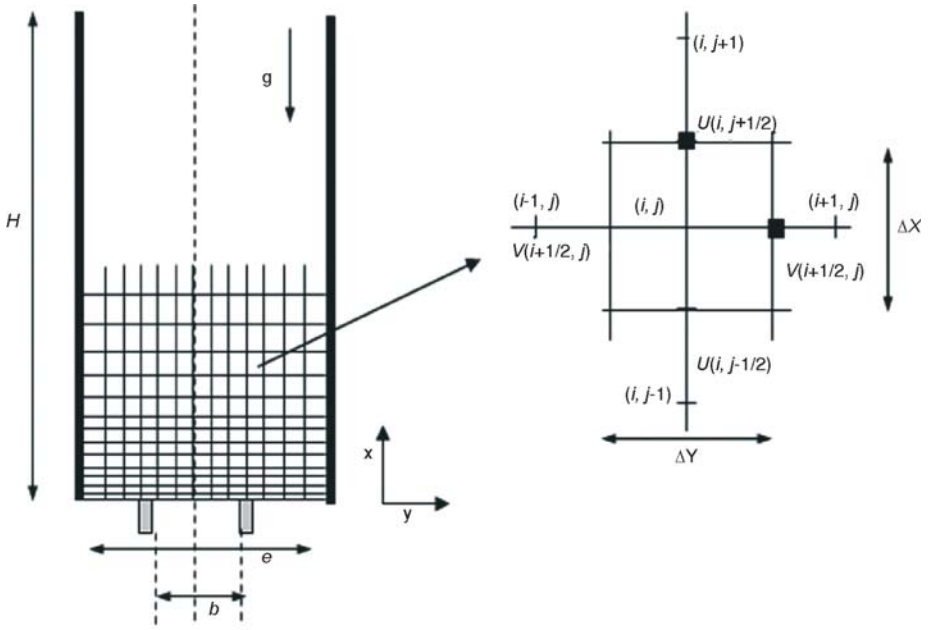

Figure 1. Physical domain and co-ordinate system

Dimensionless variables are defined by:

$$X=\frac{x}{H},\quad Y=\frac{y}{H},\quad U=\frac{u}{u_0},\quad V=\frac{v}{u_0},$$
$$P=\frac{(p+\rho g x)e^2}{\rho\alpha^2},\quad \theta=\frac{T-T_\infty}{H\phi}\lambda,\quad K=\frac{ke^2}{\alpha^2},\quad E=\frac{e^4\varepsilon}{\alpha^3} \tag{1}$$

The dimensionless governing equations for 2-D buoyancy-driven flows, with no viscous dissipation, can be written as follows:

– *continuity equation*

$$\frac{\partial U}{\partial X}+\frac{\partial V}{\partial X}=0 \tag{2}$$

– *momentum equation in X direction*

$$U\frac{\partial U}{\partial X}+V\frac{\partial U}{\partial Y}=-\frac{\partial P}{\partial X}+(\mathrm{Pr}+\mathrm{Pr_t})\left[\frac{\partial^2 U}{\partial X^2}+\frac{\partial^2 U}{\partial Y^2}\right]-\frac{2}{3}\frac{\partial K}{\partial X}+\mathrm{Ra}\,\mathrm{Pr}\,\theta \tag{3}$$

– *momentum equation in Y direction*

$$U\frac{\partial V}{\partial X}+V\frac{\partial V}{\partial Y}=-\frac{\partial P}{\partial Y}+(\mathrm{Pr}+\mathrm{Pr_t})\left[\frac{\partial^2 V}{\partial X^2}+\frac{\partial^2 V}{\partial Y^2}\right]-\frac{2}{3}\frac{\partial K}{\partial Y} \tag{4}$$

– *energy equation*

$$U\frac{\partial \theta}{\partial X}+V\frac{\partial \theta}{\partial Y}=2\left[\frac{\partial^2 \theta}{\partial X^2}+\frac{\partial^2 \theta}{\partial Y^2}\right] \tag{5}$$

– *turbulent kinetic energy equation*

$$U\frac{\partial K}{\partial X}+V\frac{\partial K}{\partial Y}=\left(\mathrm{Pr}+\frac{\mathrm{Pr_t}}{\sigma_\mathrm{k}}\right)\left(\frac{\partial^2 K}{\partial X^2}+\frac{\partial^2 K}{\partial Y^2}\right)-E+G_\mathrm{DK}+G_\mathrm{DB} \tag{6}$$

– *rate of dissipation of turbulent kinetic energy equation*

$$U\frac{\partial E}{\partial X}+V\frac{\partial E}{\partial Y}=\left(\mathrm{Pr}+\frac{\mathrm{Pr_t}}{\sigma_\varepsilon}\right)\left(\frac{\partial^2 E}{\partial X^2}+\frac{\partial^2 E}{\partial Y^2}\right)-C_1\frac{E}{K}(G_\mathrm{DB}+G_\mathrm{DK})+C_2\frac{E^2}{K} \tag{7}$$

where

$$G_\mathrm{DK}=\mathrm{Pr}_t\left(\frac{\partial U_i}{\partial X_j}+\frac{\partial U_j}{\partial X_j}\right)\frac{\partial U_i}{\partial X_j}-\frac{2}{3}K\delta_{ij}\frac{\partial U_i}{\partial X_j}\quad\text{and}\quad G_\mathrm{DB}=\frac{1}{\mathrm{Fr}}\frac{\nu_\mathrm{t}}{\mathrm{Pr_t}}\frac{\partial\theta}{\partial X} \tag{8}$$

E stands for the turbulent kinetic energy production due to shear, while G_DK is the turbulent kinetic energy production due to the mean velocity gradients, and G_DB – the turbulent kinetic energy production due to the buoyancy. The validity of the other turbulence models was tested, and the standard k-ε model seems to be the most adapted, so it is used and constants are those given by Jones *et al*. [21]: $C_1=1.44$, $C_2=1.92$, $C_3=0.7$; $C_\mu=0.09$, $\sigma_\varepsilon=1.0$, $\sigma_\mathrm{k}=1.30$, $\mathrm{Pr_t}=1.0$.

The boundary conditions are:

– at $Y=-\frac{e}{2H}$: $U=0,\ V=0,\ \left(\frac{\partial\theta}{\partial Y}\right)_p=1,\ K=0$

– at $Y=\frac{e}{2H}$: $U=0,\ V=0,\ \left(\frac{\partial\theta}{\partial Y}\right)=1,\ K=0$

– at $X = 0$

$$-\frac{e}{2H} < Y < -\frac{b}{2H} \quad \frac{\partial U}{\partial X} = 0, \quad V = 0, \quad P_g = -\frac{Q_1^2}{2}, \quad \theta = 0, \quad K = \frac{3}{2} I_t U^2$$

$$-\frac{b}{2H} < Y < -\frac{b}{2H} \quad U = 1, \quad V = 0, \quad \theta = 0, \quad K = 0.001$$

$$\frac{b}{2H} < Y < \frac{e}{2H}, \quad \frac{\partial U}{\partial X} = 0, \quad V = 0, \quad P_g = \frac{Q_1^2}{2}, \quad \theta = 0, \quad K = \frac{3}{2} I_t U^2$$

– at $X = 1$: $\frac{\partial U}{\partial X} = \frac{\partial V}{\partial X} = \frac{\partial \theta}{\partial X} 0, \quad P = 0, \quad K = \frac{3}{2} I_t U^2 \quad E = \frac{2eK^{0.5}}{b}$

where

$$Q_1 = \int_{b/2H}^{e/2H} U \mathrm{d}Y, \quad Q_3 = \int_{-e/2H}^{-b/2H} U \mathrm{d}Y$$

and

$$Q_2 = \int_{-b/2H}^{b/2H} U \mathrm{d}Y$$

and I_t is the turbulence intensity.

The governing equations reported above are discretized on a staggered, non-uniform Cartesian grid using a finite volumes procedure. In this method, for stability considerations, scalar quantities P, θ, K, and E are calculated at the centre (i, j) of the cells whereas the velocity components (U and V) are computed on the faces of the cells $(i, j \pm 1/2)$, $(i \pm 1/2, j)$.

Results and discussion

Preliminary tests were carried out to verify the accuracy of the numerical solution, the computations were performed first for a simple channel – *i. e.* without gas injection from the nozzle – and numerical results were compared with the experimental ones published by Auletta *et al.* [27] (fig. 2). The resulting free convection problem was simulated with $L/2e = 2.5$ and, which corresponds to a Rayleigh number equal to $1.16 \cdot 10^{11}$. The Prandtl number is 0.71 (air). The local wall temperature is reported in fig. 2. Differences between measurements and numerical predictions are very low and they mainly concern the highest part of the channel. This may be due to the fact that there were some heat losses caused by insufficient thermal insulation in experiments. Moreover, the im- posed wall heat flux was not uniform because of the space between two successive heaters. At least, the use of thermocouples also modifies the flow structure, especially in the vicinity of the plates.

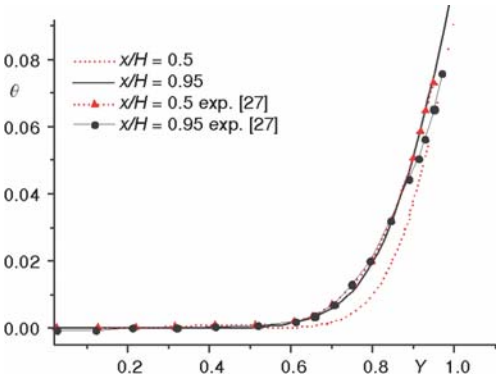

Figure 2. Local temperature evolution: steady flow without injection; comparison with experiment

Results for the parametric analysis are carried out for air, Pr = 0.71, where the Rayleigh number ranges from $2.57 \cdot 10^{10}$ (boundary layers connected) to $5.15 \cdot 10^{12}$ (the boundary layers remain separate till the end of the channel) and for a channel aspect ratio L/e = 12.5 and two Reynolds number based on the velocity of the jet

at the nozzle exit $Re = 3 \cdot 10^3$ and $Re = 2 \cdot 10^4$. The two values of the Reynolds number are chosen so that for the first value ($Re = 3 \cdot 10^3$) the natural convection due to the wall heating is dominant, for the second value ($Re = 2 \cdot 10^4$) forced convection is dominant. Computations deals with both symmetrically and asymmetrically heated channel. The imposed heat flux and the jet velocity on the heat transfer enhancement are evaluated. Based on the velocity and the temperature results, mass flow rate and the average Nusselt number are analyzed.

Figure 3 shows the evolution of the velocity at the channel exit section for various walls heating. Note that heating asymmetry affects the velocity profile for $Re = 3 \cdot 10^3$, fig.3(a). A fully developed velocity distribution is not expected and was not obtained at the exit of the channel. The velocity distribution reveals steep gradients near the walls and an increase in boundary layer thickness with distance along the channel. Conversely, for high Reynolds number $Re = 2 \cdot 10^4$, the velocity profile is the same for all imposed heat fluxes, fig. 3(b). This is due to the dominant effect of the external flow. For these imposed conditions buoyancy has a little effect on velocity distributions.

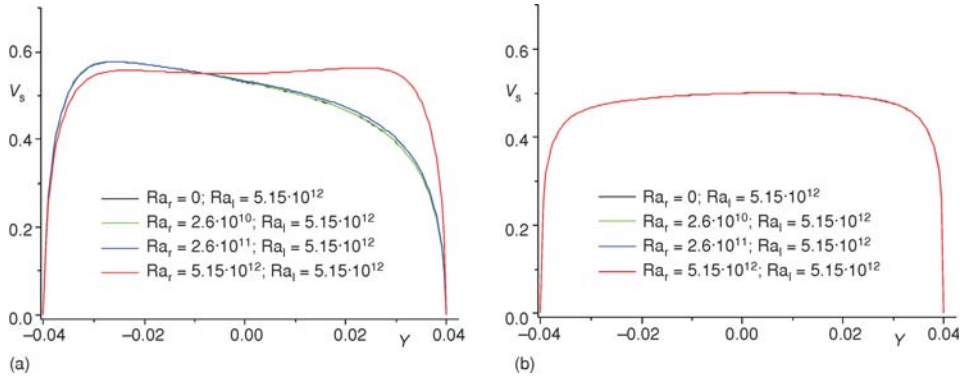

Figure 3. Stream wise evolution of the velocity at the channel exit section; (a) Re = 3000, (b) Re = 20000

We notice in fig. 4 that the velocity in the vicinity of the hot plate is increased for the asymmetrically heating compared to the symmetrical case. This can be explained by the boundary layers interaction, largely studied in the literature [29]. Indeed for significant Rayleigh numbers the channel behaves like two independent plates, while for low Rayleigh numbers, the velocity gradient becomes very large and the boundary layers interact. In the case of the asymmetrical heating the boundary layer in the locality of the lowest Rayleigh number plate widens in spite of hot plate boundary layer of low thick-

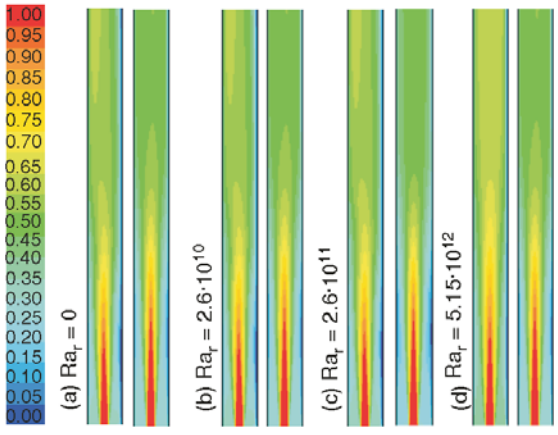

Figure 4. Velocity development in the channel; $Ra_l = 5.15 \cdot 10^{12}$, $Re = 3 \cdot 10^3$ (left); $Re = 2 \cdot 10^4$ (right) (color image see on our web site)

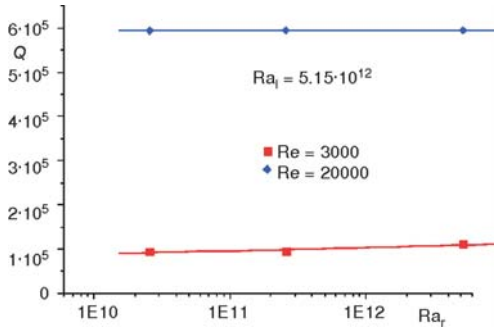

Figure 5. Mixed convection drived flow rate in the entrance section

ness; what generates an additional acceleration of the fluid in the vicinity of the warm plate (fig. 4).

The non-dimensional induced mass flow rate at both side of the jet defined as $Q = Q_1 + Q_3$ shown in fig. 5 is the dimensionless mass flow rate, as a function of the left wall Rayleigh number. For high Reynolds number $Re = 2 \cdot 10^4$, the induced mass flow rate is independent of the imposed heat flux. For low Reynolds number $Re = 3 \cdot 10^3$, a sensible mass flow rate increment is observed; this is clearly caused by a greater induced natural convection flow.

For asymmetrically heated channel the induced mass flow rate is not similar in both side of the channel for low Reynolds numbers; however it remains similar even when imposed heat fluxes are not equal for highest jet velocities. When the Reynolds number increases, a sensible mass flow rate increment is observed; this is clearly caused by a great driving force. This confirms that the walls' heating affects the flow only for low Reynolds numbers and that the flow is due in large majority to the drive by the jet and for important Reynolds. For low Reynolds numbers, the walls' heating involves the flow: the strength of the natural convection flow is more important than the jet's drive.

Skin friction evolution along the channel wall's are reported on fig. 6. Note that the difference are seen only for low Reynolds number, however a light difference is seen at the highest half of the channel for $Re = 2 \cdot 10^4$. For low Reynolds number, increasing the right plate heat fluxes increases the skin friction. Further, it is important to observe that the wall submitted to an equal heat flux do not behave at the same manner for different imposed heat fluxes at the opposite wall.

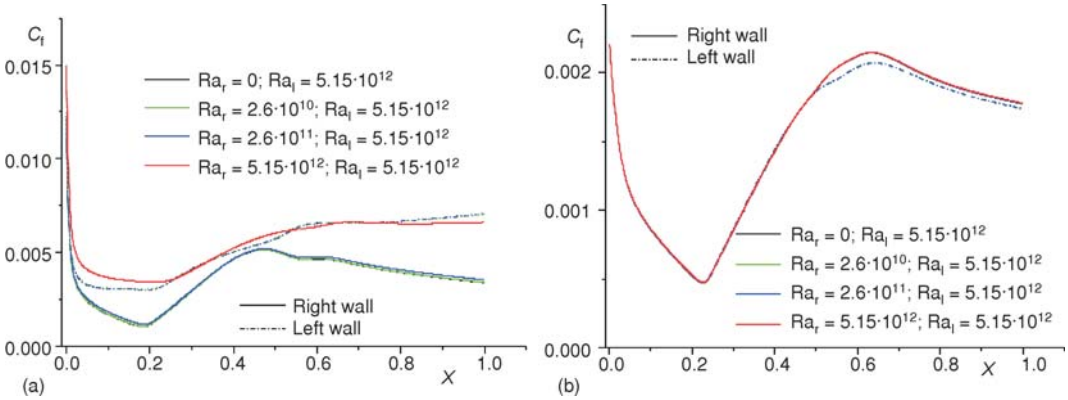

Figure 6. Streamwise evolution of the local friction coefficient; (a) Re = 3000, (b) Re = 20000

This can be explained by the difference of the velocity in the vicinity of these walls due to the change on the boundary layer width for diverse configurations.

The developing of the flow depends not only on the heat flux imposed on the left plate but also on the right plate, the right boundary layer whether interacts with the left one, or re-

mains separate. This interaction influences the flow velocity in the boundary layer and consequently the skin friction. The boundary layer thinned, velocity in the boundary layer decreases, turbulence becomes moderate, which involve a decrease in the friction coefficient. For Re = $= 2 \cdot 10^4$, the flow development is controlled by forced convection, macroscopic agitation is added to molecular agitation thus ensuring a significant momentum transport between the various fluid layers. The influence of the heating asymmetry is seen only far from the jet impact zone: the skin friction decreases for lowest Rayleigh numbers.

We show in fig. 7 the dimensionless wall temperature profile for the four cases that we have taken into consideration. In all of the cases the highest value of maximum wall temperature is attained for the natural convection configuration. These profiles allow deducing that the introduction of the jet enhances the transfer between the flow and the walls whatever the value of the Reynolds number is. In the vicinity of the entry the parietal temperature increases according to the longitudinal distance. The maximum wall temperature is attained right before the impact zone. This peak is due to the containment of the flow evacuated by natural convection on both sides of the jet. The maximum temperature zone corresponds to the zone where were formed the recirculation currents. This swirling causes the disturbance of the boundary layer (heat insulator) hence, the thickness of the latter decreases. So the wall-fluid exchange increases. This fluid being confined in this zone warms up more and transmits its heat consequently to the plate. The heat flux becomes thus very intense. We note that the heating dissymmetry influences the two channel walls. The lowest plate (right plate) temperature increases and goes beyond the impact zone under the hot plate (left) effect. This occurs due to the change of the width of the boundary layer.

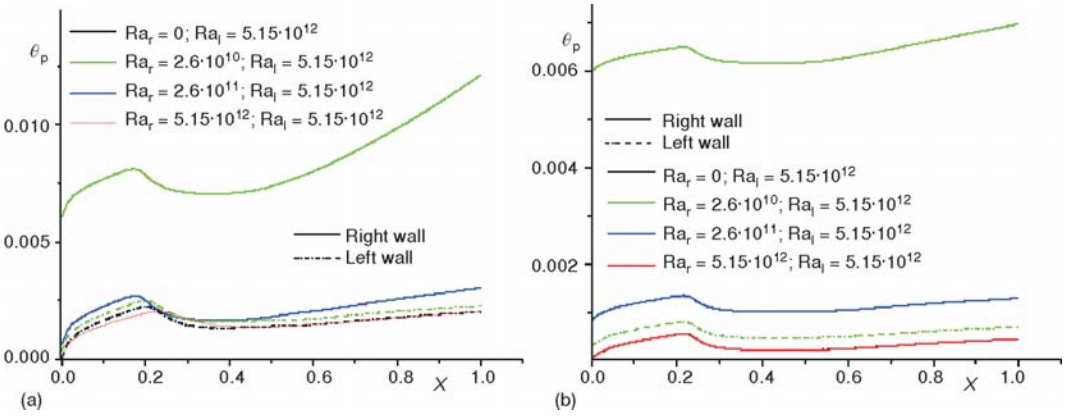

Figure 7. Longitudinal wall temperature; (a) Re = 3000; (b) Re = 20000

For low Reynolds numbers ($Re = 3 \cdot 10^3$) the jet impact zone is not located at the same ordinate for the two channel walls, the intensity of natural convection flow depends on the heat flux intensity, for low Reynolds numbers, the natural convection flow is of the same intensity as the jet, so it modifies the characteristics of the forced convection: the penetration of the jet is more important and the impact zone is hustled in the flow direction. For $Re = 2 \cdot 10^4$ the jet impact zone is located at the same ordinate, in fact the driven flow is primarily caused by the jet.

The effect of the channel heating on the local Nusselt number is illustrated in fig. 8.

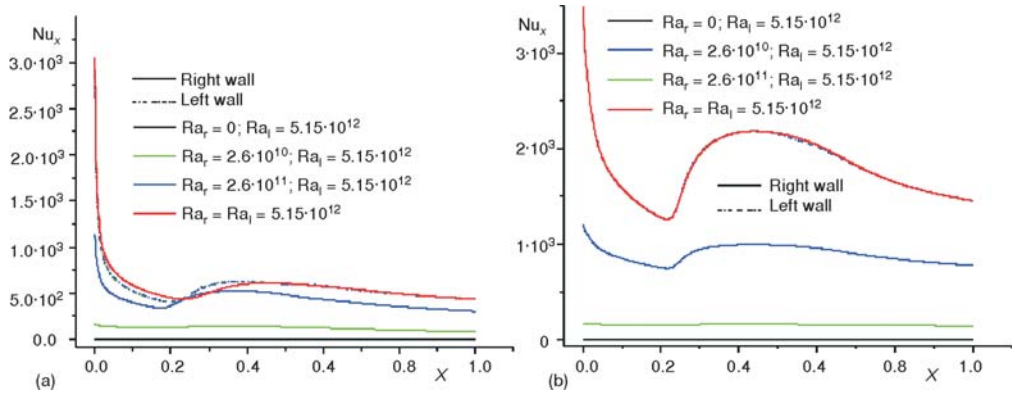

Figure 8. Local Nusselt number; (a) Re =3000, (b) Re = 20000

For Re = $3 \cdot 10^3$, as the right wall Rayleigh number increases, the maximum transfer point moves downstream. And then decreases very gradually from this point. At the downstream of the channel, for lowest Rayleigh numbers, the curves become flat up to the end. Additionally, for the cases of asymmetrical heating, the peak of the curves of the local Nusselt number is located closer to the entrance region; this is due to the change of the jet impact zone. It implies that asymmetrical heating benefits to the hot wall heat transfer enhancement only in the impact zone: the peak is larger and located more closely to the entrance region. For Re = $2 \cdot 10^4$, no change on the heat transfer behaviour of the left wall. The average Nusselt number increases according the right plate Rayleigh number (fig. 9). The left wall Nusselt number remain constant, however the right one increases. Predictable result since we apply the same heat flux on the right plate, and the variation in the local Nusselt number of the left wall is not important and concerns only the impact zone for low Reynolds number.

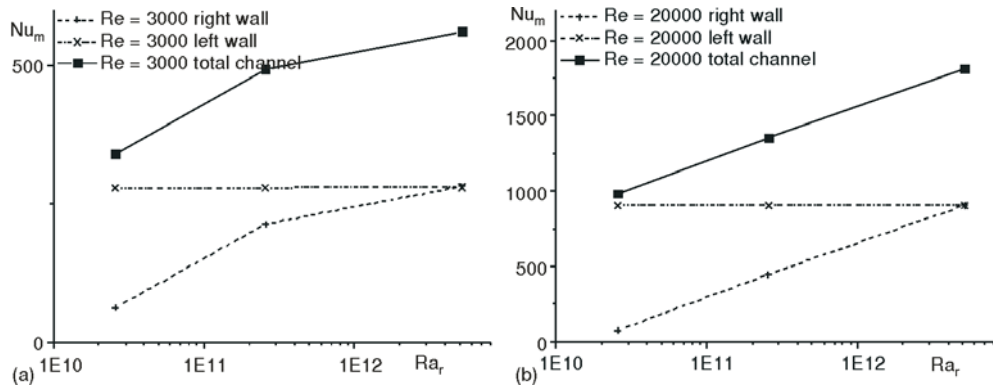

Figure 9. Average Nusselt number according to the right wall Rayleigh number; (a) Re = 3000, (b) Re = 20000

Conclusions

In this study, combined forced and natural convection has been performed, the mixed convection occurs between two vertical walls asymmetrically heated by a constant heat flux. The mixed flow is obtained by using an ascending jet located at the entry section of the channel.

Flow features, temperature and velocity are computed in order to evaluate the heat transfer. Computations were carried out for two Reynolds numbers $Re = 3 \cdot 10^3$ and $Re = 2 \cdot 10^4$. It is observed that the flow behaviour is different for the two cases. The buoyancy influence is noticeable for $Re = 3 \cdot 10^3$, so it have a significant impact on the flow quantities. In contrast to $Re = 2 \cdot 10^4$, the flow is mainly driven by the mean pressure gradient, the flow depends in great majority on the forced convection flow. The heat flux dissymmetry influences mainly the induced mass flow rate and the local quantities such as the velocity, the wall temperature and the local Nusselt number. The average Nusselt number remains unchanged. However we note a change on the local Nusselt number distribution. This can be explained by the fact that the change in local Nusselt number is not important and concerns only the impact zone.

Nomenclature

- b – width of the nozzle, [m]
- E – dimensionless rate of dissipation of turbulent kinetic energy, [–]
- e – width of the channel, [m]
- Fr – Froude number [$= u^2/g\beta(T - T_\infty)b$, [–]
- g – gravitational acceleration, [ms^{-2}]
- H – length of the channel, [m]
- h – local heat transfer coefficient, [$Wm^{-2}K^{-1}$]
- K – dimensionless turbulent kinetic energy, [–]
- k – turbulent kinetic energy, [m^2s^{-2}]
- Nu – Nusselt number ($= hx/\lambda$), [–]
- P – dimensionless pressure, [–]
- p – pressure, [Pa]
- Pr – Prandtl number ($= \mu c_p/\lambda$), [–]
- $Q_{1,3}$ – dimensionless mass flow rate at the inlet section of the channel [$= \dot{m}_1/(e - b)\alpha\rho$], [–]
- Q_2 – dimensionless mass flow rate at the exit section of the nozzle, [–]
- Ra – Rayleigh number ($= g\beta H^4\varphi/\lambda\alpha\nu$), [–]
- Re – Reynolds number, ($= bu_0/\nu$) [–]
- T – temperature, [K]
- U,V – dimensionless velocity components along X and Y axis, respectively, [–]
- u, v – velocity components along x and y axis, respectively, [ms^{-1}]
- X, Y – dimensionless co-ordinates, [–]
- x, y – co-ordinates, [m]

Greek symbols

- α – thermal diffusivity, [m^2s^{-1}]
- ε – turbulent kinetic energy dissipation, [m^2s^{-3}]
- Φ – wall heat flux, [Wm^{-2}]
- λ – thermal conductivity, [$Wm^{-1}K^{-1}$]
- μ – dynamic viscosity, [$kgm^{-1}s^{-1}$]
- ν – kinematic viscosity, [m^2s^{-1}]
- ρ – fluid density, [kgm^{-3}]
- θ – dimensionless temperature, [–]

Subscripts

- l – left wall
- m – average
- p – wall value
- r – right wall
- x – local value
- ∞ – external (ambient conditions value)

References

[1] Sunden, B., Comini G., Computational Analysis of Convection Heat Transfer, WIT Press, Southampton, UK, 2000
[2] Peterson, G. P., Ortega, A., Thermal Control of Electronic Equipment and Devices, *Advances in Heat Transfer, 20* (1990), pp. 181-314
[3] Campo, A., Manca, O., Morrone, B., Numerical Analysis of Partially Heated Vertical Parallel Plates in Natural Convective Cooling, *Numerical Heat Transfer, Part A: Applications, 36* (1999), 2, pp. 129-151
[4] Bar-Cohen, A., Rohsenow, W. M., Thermally Optimum Spacing of Vertical Natural Convection Cooled Parallel Plates, *Journal of Heat Transfer, 106* (1984), 1, pp. 116 -123
[5] Betts, P. L., Dafa'nela, A. A., Turbulent Buoyant Air Flow in a Tall Rectangular Cavity, *Proceedings* (ASME HTD) Winter Annual Meeting, New York, USA, Vol. 60, 1986, p. 83
[6] Cheung, F. B., Sohn, D.Y., Numerical Study of Turbulent Natural Convection in an Innovative Air Cooling System, *Numerical Heat Transfer, Part A: Applications, 16* (1989), 4, pp 467- 487
[7] Gebhart, B., *et al*., Buoyancy-Induced Flows and Transport, Hemisphere, Washington DC, 1987

[8] Kim, S. J., Lee, S. W., Air Cooling Technology for Electronic Equipment, CRC Press, Boca Raton, Fla., USA, 1996
[9] Bejan, A., Shape and Structure from Engineering to Nature, Cambridge University Press, New York, USA, 2000
[10] Ledezma, G. A., Bejan, A., Optimal Geometric Arrangement of Staggered Vertical Plates in Natural Convection, *ASME Journal of Heat Transfer, 119* (1997), 4, pp. 700-708
[11] Sathe, S., Sammakia, B., A Review of Recent Developments in some Practical Aspects of Air-Cooled Electronic Packages, *ASME Journal of Heat Transfer, 120* (1998), 4, pp. 830-839
[12] Bejan, A., Da Silva, A. K., Lorente, S., Maximal Heat Transfer Density in Vertical Morphing Channels with Natural Convection, *Numerical Heat Transfer, Part A: Applications, 45* (2004), 2, pp. 135-152
[13] Auletta, A., *et al*., Heat Transfer Enhancement by the Chimney Effect in a Vertical Isoflux Channel, *International Journal of Heat and Mass Transfer, 44* (2001), 22, pp. 4345-4357
[14] Da Silva, A. K., Gosselin, L., Optimal Geometry of L- and C-Shaped Channels For Maximum Heat Transfer Rate in Natural Convection, *International Journal of Heat and Mass Transfer, 48* (2005), 3-4, pp. 609-620
[15] Andreozzi, A., Campo, A., Manca, O., Compounded Natural Convection Enhancement in a Vertical Parallel-Plate Channel, *International Journal of Thermal Sciences, 47* (2008), 6, pp. 742-748
[16] Hall, W. B., Jackson, J. D., Laminarization of a Turbulent Pipe Flow by Buoyancy Forces, ASME paper, No. 69-HT-55, 1969
[17] Jackson, J. D., Hall, W. B., Influence of Buoyancy on Heat Transfer to Fluids Flowing in Vertical Tubes under Turbulent Conditions, in: Turbulent Forced Convection in Channels and Bundles (Eds. S. Kakac, D. B. Spalding), Hemisphere Publishing, New York, USA, 1979
[18] Jiulei, W., Jiankang, L., Jackson, J. D., A Study of the Influence of Buoyancy on Turbulent Flow in a Vertical Plane Passage, *International Journal of Heat and Fluid Flow, 25* (2004), 3, pp. 420-430
[19] Jackson, J. D., Cotton, M. A., Axcell, B. P., Studies of Mixed Convection in Vertical Tubes, *International Journal of Heat and Fluid Flow, 10* (1989), 1, pp. 2-15
[20] Jackson, J. D., Studies of Buoyancy Influenced Turbulent Flow and Heat Transfer in Vertical Passages, *Proceedings*, 13th International Heat Transfer Conference, Sydney, Australia, 2006
[21] Nakajima, K., *et al*., Buoyancy Effects on Turbulent Transport in Combined Free and Forced Convection Between Vertical Parallel Plates, *International Journal of Heat and Mass Transfer, 23* (1980), 10, pp. 1325-1336
[22] Miyamoto, M., *et al*., Turbulent Free Convection Heat Transfer from Vertical Parallel Plates, in: Heat Transfer (Eds. C. L. Tien, V. P. Carey, J. K. Ferrell), Hemisphere, Washington DC, 1986
[23] Fedorov, A. G., Viskanta, R., Turbulent Natural Convection Heat Transfer in an Asymmetrically Heated Vertical Parallel Plate Channel, *International Journal of Heat Mass Transfer, 40* (1997), 16, pp. 3849-3860
[24] Versteegh, T. A. M., Nieuwstadt, F. T. M., Turbulent Budgets of Natural Convection in an Infinite, Differentially Heated, Vertical Channel, *International Journal of Heat and Fluid Flow, 19* (1998), 2, pp.135-149
[25] Versteegh, T. A. M., Nieuwstadt, F. T. M., A Direct Numerical Simulation of Natural Convection Between Two Infinite Vertical Differentially Heated Walls Scaling Laws and Wall Functions, *International Journal of Heat and Mass Transfer, 42* (1999), 19, pp. 3673-3693
[26] Dalbert, A. M., Penot, F., Peube, J. L., Laminar Natural Convection in a Vertical Heated Channel by a Constant Flux (in French), *International Journal of Heat and Mass Transfer, 24* (1981), 9, pp. 1463-1473
[27] Auletta, A., Manca, O., Heat and Fluid Flow Resulting from the Chimney Effect in a Symmetrically Heated Vertical Channel with Adiabatic Extensions, *International Journal of Thermal Sciences, 41* (2002), 12, pp. 1101-1111
[28] Penot, F., Dalbert, A. M., Mixed Forced and Natural Convection in a Vertical Thermosiphon Heated by a Constant Flux (in French), *International Journal of Heat and Mass Transfer, 26* (1983), 11, pp. 1639-1647
[29] Bar-Cohen, A., Rohsenow, W. M., Thermally Optimum Spacing of Vertical Natural Convection Cooled Parallel Plates, *Journal of Heat Transfer, 106* (1984), 1, pp. 116-123

Paper submitted: April 3, 2009
Paper revised: January 12, 2012
Paper accepted: January 16, 2012